

PbSe nanocrystal/conducting polymer solar cells with an infrared response to 2 micron

Xiaomei Jiang^{a)}

Nanotech Institute, University of Texas at Dallas, Richardson, Texas 75083; and Physics Department, University of South Florida, Tampa, Florida 33620

Richard D. Schaller^{b)}

Chemistry Division, Los Alamos National Laboratory, Los Alamos, New Mexico 87545

Sergey B. Lee

Nanotech Institute, University of Texas at Dallas, Richardson, Texas 75083; and Plextronics, Inc., Pittsburgh, Pennsylvania 15238

Jeffrey M. Pietryga and Victor I. Klimov

Chemistry Division, Los Alamos National Laboratory, Los Alamos, New Mexico 87545

Anvar A. Zakhidov

Nanotech Institute, University of Texas at Dallas, Richardson, Texas 75083; and Physics Department, University of Texas at Dallas, Richardson, Texas 75083

(Received 28 February 2007; accepted 3 May 2007)

We investigated the photovoltaic response of nanocomposites made of colloidal, infrared-sensitive, PbSe nanocrystals (NCs) of various sizes and conjugated polymers of either regioregular poly (3-hexylthiophene) (RR-P3HT) or poly-(2-methoxy-5-(2-ethylhexoxy)-1,4-phenylene vinylene) (MEH-PPV). The conduction and valence energy levels of PbSe NCs were determined by cyclic voltammetry and revealed type II heterojunction alignment with respect to energy levels in RR-P3HT for smaller NC sizes. Devices composed of NCs and RR-P3HT show good diode characteristics and sizable photovoltaic response in a spectral range from the ultraviolet to the infrared. Using these materials, we have observed photovoltaic response at wavelengths as far to the infrared as 2 μm (0.6 eV), which is desirable due to potential benefits of carrier multiplication (or multi-exciton generation) from a single junction photovoltaic. Under reverse bias, the devices also exhibit good photodiode responses over the same spectral region.

I. INTRODUCTION

Semiconductor nanocrystals (NCs) have several properties that make them attractive for use as the photoactive material in solar cells. First, the material band gap can be tuned over a large energy range simply via synthetic control over the NC-size.¹ NCs that have an absorption onset in the near- to mid-infrared (IR) will also strongly absorb solar photons of higher energy. Furthermore, it has been found that NCs efficiently generate multiple excitons upon absorption of single photons of sufficient energy via carrier multiplication.^{2,3} Using this process one can appreciably increase the photovoltaic power conversion efficiency above the Shockley–Queisser apparent

thermodynamic limit.^{4,5} Solution-processable materials such as semiconductor NCs combined with conjugated polymers can promote efficient charge transfer and make possible the production of low-cost, high-efficiency solar cells.

NCs mixed with conducting polymers have been actively studied following the work of Greenham, Alivisatos, and co-workers.^{6–8} Progress in this direction has been made via study of the NC-polymer composite morphology⁹ by using polymers that are functionalized to attach to NC surfaces¹⁰ and by improvement of electron transport via incorporation of branched or elongated nanoparticles.^{8,11} Further improvements in solar cell performance can be obtained from more effective collection of photons from the low-energy portion of the solar spectrum, which can be accomplished by utilizing narrow gap materials with an absorption onset in the IR. Additional improvements can be obtained through more effective utilization of the ultraviolet (UV) light via effects such as

Address all correspondence to these authors.

^{a)}e-mail: xjiang@cas.usf.edu

^{b)}e-mail: rdsx@lanl.gov

DOI: 10.1557/JMR.2007.0289

multiple exciton generation.^{2,3,12,13} The latter also requires the use of IR materials because the effect of multi-exciton generation causes the optimal power conversion efficiency of a single junction photovoltaic to shift to band gap of $\sim 0.35\text{--}0.45$ eV⁵ (depending upon the position of the carrier multiplication threshold with regard to the semiconductor energy gap) in contrast to ~ 1.1 eV in the absence of this effect.⁴

The development of high-quality IR-absorbing NCs^{14–17} promises to expand the spectral responsivity of photovoltaic cells to the IR region of the solar spectrum, which is inaccessible with existing organic materials. Unique challenges are faced in such work, however, because type II heterojunction alignment (i.e., “staggered” configuration of band-edge energies, see Fig. 1) of the material energy levels becomes difficult for small NC band gaps, i.e., for large NC sizes. Here we demonstrate photovoltaic performance in PbSe NC-conjugated polymer composites for photon energies as low as 0.6 eV (2 μm).

Near-infrared photovoltaic and photodiode performance have been demonstrated in devices consisting of PbS NCs and conducting polymers^{18–21} (as well as TiO₂).²² In our earlier work, we demonstrated photovoltaic performance from nanocomposites of regioregular poly-(3-hexylthiophene) (RR-P3HT) and PbSe NCs,²³ which was the first report about photovoltaic effect under solar AM1.5 illumination with intensity 100 mW/cm² in such a system. Recently, similar results were presented in Ref. 24, which describes a device structure made of only one size of (6 nm) PbSe NCs. The reported device showed the following performance: the open circuit volt-

age $V_{oc} = 0.37$ V, the short-circuit current density $J_{sc} = 1.08$ mA/cm², the fill factor $FF = 0.37$, and a power conversion efficiency of 0.14% under 1 sun illumination. Photodiode response has previously been reported for composites of PbSe NCs and MEH-PPV.²⁵

In our present report, we perform a systematic comparative analysis of nanocomposites made of PbSe NCs of several different sizes (4–10 nm diameter) and combined with either poly (2-methoxy-5-(2-ethylhexoxy)-1,4-phenylene vinylene) (MEH-PPV) or RR-P3HT as a hole-conducting material. Specifically, we analyze the photovoltaic performance of these structures in the context of our results for energy-level alignment in PbSe NC/polymer systems obtained through direct electrochemical measurements. PbSe NCs, which have a band gap that is size-tunable from ~ 0.3 to 1.5 eV,^{14,15} were first studied using cyclic voltammetry (CV) to determine the positions of the band edge conduction and valence energy levels. NCs were then combined in solution with either RR-P3HT or MEH-PPV. We find that thin-film RR-P3HT/PbSe-NC nanocomposite cells show very clear diode characteristics and sizable photovoltaic response with an open circuit voltage of $\sim 0.3\text{--}0.4$ V and short circuit current density of ~ 0.2 mA/cm² in the best device, under 100 mW/cm² (AM1.5) solar illumination conditions.

Photovoltaic performance at IR wavelengths indicates that photoinduced charge transfer takes place between the NC and polymer components. Photocurrent under reverse bias is significantly enhanced in the IR (to $J_{ph} \sim 2$ mA/cm²), which indicates that the RR-P3HT/PbSe NC devices can also be used as IR photodetectors. Spectroscopic studies of photoresponse over a wide spectral range are presented.

II. EXPERIMENTAL

The NCs used in this work were synthesized according to literature methods^{14,15} and in some instances were purchased from Evident Technologies (Troy, NY). NCs were precipitated three times out of hexane by addition of methanol to remove excess ligand as well as some amount of surface bound ligand. A blend containing a 6:1 weight ratio of the NCs to polymer was dissolved in chloroform and then spin-coated ($\sim 100\text{--}130$ nm thick layer) onto indium-tin-oxide (ITO)-coated glass substrates (<15 ohms/sq with $\sim 85\%$ light transmission) that had been UV-ozone cleaned and coated with poly(3,4-ethylenedioxythiophene) poly(styrenesulfonate) (PEDOT-PSS) hole transporter [Fig. 1(a)]. Four devices were fabricated on each substrate, each having an area of ~ 0.09 cm². A 100-nm-thick aluminum cathode was then deposited under high vacuum. Current–voltage measurements were performed with a Keithley 236 source-measure unit (Cleveland, OH). A ThermoOriel 300 W solar simulator

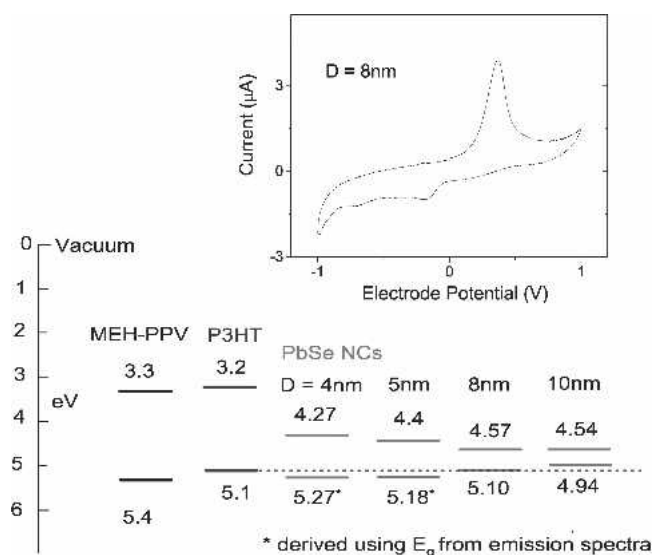


FIG. 1. Energy-level positions of MEH-PPV, P3HT, and PbSe NCs of different sizes measured by electrochemical cyclic voltammetry. The dashed line shows the HOMO level of P3HT. Inset shows one example of such cyclic voltammogram recorded at a sweep rate of 20 mV/s for PbSe NCs with diameter of 8 nm.

with AM1.5 filter and light intensity calibrated at 100 mW/cm^2 was used as the light source for power conversion efficiency measurements. Results of the latter measurements were not corrected for spectral mismatch.

To construct devices capable of producing a photovoltaic response, we first needed to determine the position of the ionization potential I_p and electron affinity E_a of each size PbSe NCs. Previous cyclic voltammetry (CV) studies of PbSe NCs were conducted in Refs. 26 and 30. Specifically, Wehrenberg and Guyot-Sionnest²⁶ have shown that both electrons and holes can be injected into PbSe NCs. In our CV studies, to quantify the positions of electronic levels, we used thin films of PbSe NCs, which were drop cast from hexane solution onto a 3-mm-diameter platinum working electrode and dried in a vacuum oven at 70°C for 2 h before loading them into the electrochemical cell. Glassy carbon was used as the counter electrode, and the reference electrode was Ag/AgNO₃ (0.1 M AgNO₃ in acetonitrile). All measurements were carried out in a nitrogen-filled dry box to minimize exposure to oxygen and water. Similar CVs were obtained using a gold electrode. The energy levels of PbSe NCs were estimated using normal hydrogen electrode (NHE) potential and a reference ferrocene/ferricinium (Fc/Fc⁺) redox couple.²⁷

III. RESULTS AND DISCUSSION

Figure 1 shows the schematic energy levels of PbSe NCs as well as the levels of MEH-PPV and RR-P3HT (from Refs. 28 and 29). It can be seen that there is a large energy offset between the conduction bands of the NC and polymer components, and there is a much smaller offset between the valence bands. Because the energy levels of the NCs change with size, type II alignment (and thus photovoltaic performance) is expected to be present only for smaller NCs when combined with RR-P3HT. This loss of type II alignment will limit the onset of IR response that is possible with this combination of materials. Furthermore, type II alignment is not expected for any of the NC sizes in combination with MEH-PPV, although size dispersion in the NC-component and variation in polymer conjugation length can possibly allow for some photovoltaic response. From the relative positions of the energy levels, better photovoltaic performance is expected for nanocomposites made of PbSe NCs and RR-P3HT in comparison to PbSe NCs with MEH-PPV.

Figure 2(b) shows the current–voltage characteristics of a device [with the architecture shown in Fig. 2(a)] made of RR-P3HT and 8-nm-diameter PbSe NCs. The V_{oc} for this device was 0.34 V, J_{sc} was 0.2 mA/cm^2 , and the power conversion efficiency was 0.04% under AM1.5, 100 mW/cm^2 , simulated solar illumination (the efficiency increased to 0.14% under 10 mW/cm^2 light intensity). Figure 2(c) shows a comparison of device

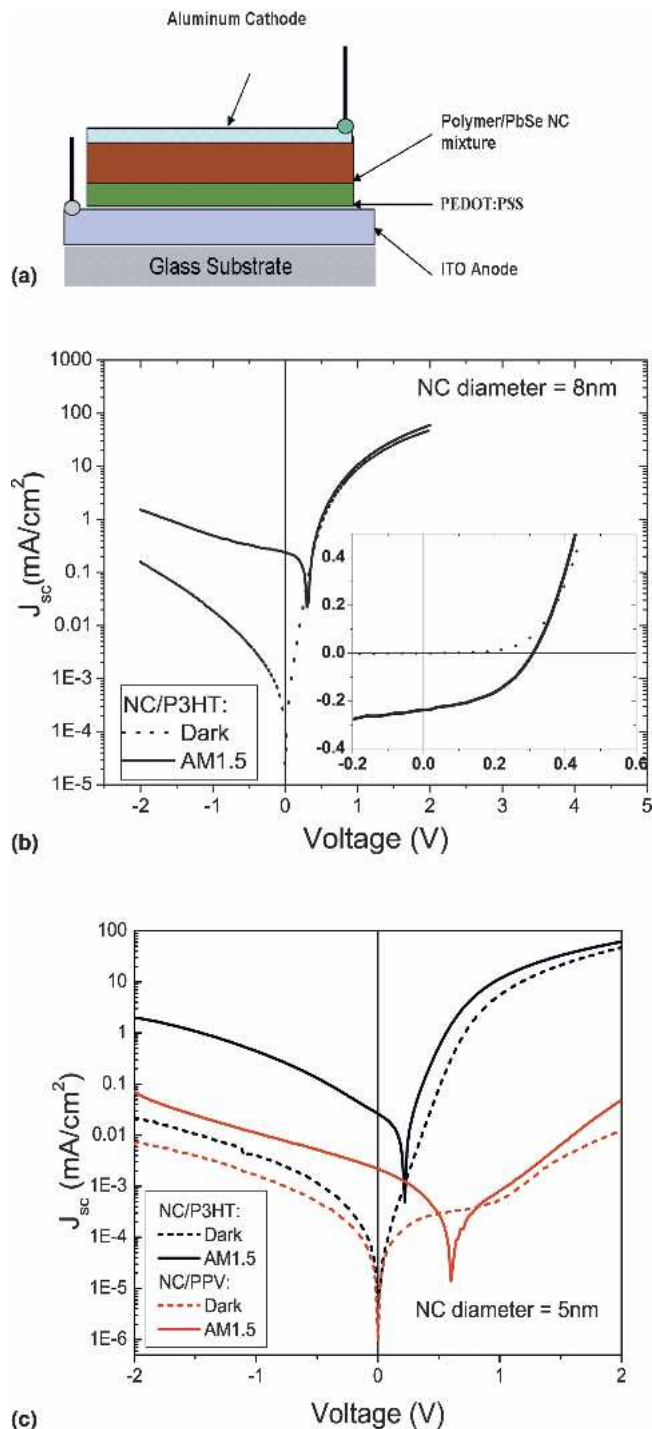


FIG. 2. Comparison of ITO/PEDOT:PSS/Polymer:PbSe NCs/Al (1:6) composites of PbSe NCs with either P3HT or MEH-PPV: (a) device architecture and (b) current–voltage characteristics of a device made of P3HT:PbSe NCs ($E_g = 0.67 \text{ eV}$, 8 nm NC size), with open circuit voltage $V_{oc} = 0.32 \text{ V}$, short circuit current density $J_{sc} = 0.24 \text{ mA/cm}^2$, fill factor of 0.43, and a power conversion efficiency of 0.04%. The inset shows a zoom-in of the region of interest for photovoltaic performance. (c) Current–voltage characteristics in the dark (dashed lines) and under AM1.5 illumination (solid lines) for devices made with P3HT:PbSe NC (black) and MEH-PPV:PbSe NC (red), PbSe NC size ($E_g = 0.78 \text{ eV}$, 5 nm NC diameter) is the same for both devices.

performance for composites made of a fixed NC size (5-nm-diameter, band gap 0.78 eV) and either RR-P3HT (black) or MEH-PPV (red); the weight ratio of the NCs to the polymer was 6:1. It can clearly be seen that the device incorporating RR-P3HT shows significantly better diode characteristics and a larger photoresponse than a similar device made of NCs and MEH-PPV, which is consistent with the energy level alignment shown in Fig. 1.

To investigate the photoresponse originating only from PbSe NCs, we illuminated the devices with a 100 mW, 830 nm continuous wave laser. Figure 3 shows the dependence of (a) J_{sc}^{norm} and (b) V_{oc} on NC band gap. To account for differences in the amount of light absorbed in different devices (due, for example, to differences in their thickness), we normalize J_{sc} by the device absorptivity and also introduce a correction factor, which accounts for variations in device reflectivity. [Normalized short circuit current density (J_{sc}^{norm}) was calculated by dividing the measured short circuit current density by the device absorptivity (A). The latter quantity was determined from the expression $A = (I - T - R)/I$, where I , T , and R are the incident, transmitted, and reflected light intensities, respectively. The scattered portion of incident light was not taken into account in the calculation of A .] The data in panel (a) clearly show that the photocurrent has an onset at $E_g \sim 0.6$ eV (NC diameter is 8 nm), which is consistent with the energy diagram shown in Fig. 1. Upon absorption of an incident photon by an NC, the photogenerated exciton dissociates into an electron and hole at the polymer/NC interface. The electron remains in the NC and is transported to the Al electrode via hopping from the NC to the NC.³¹ The hole is

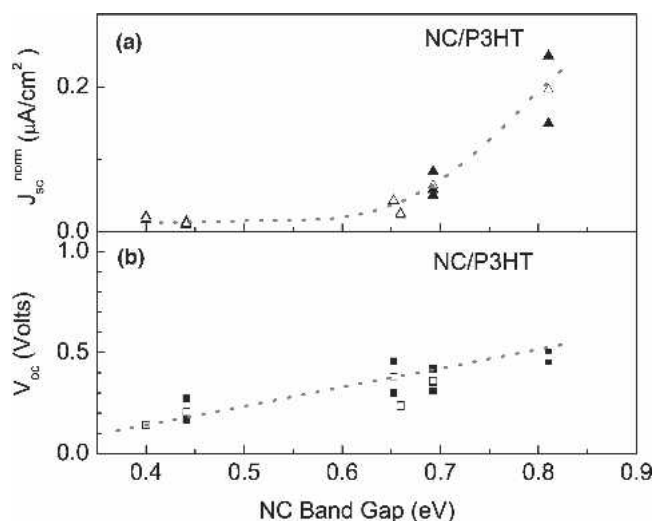


FIG. 3. (a) J_{sc}^{norm} and (b) V_{oc} dependence on PbSe NC band gap measured for several devices made from the RR-P3HT/PbSe NC blend. Excitation is from an 830-nm laser diode with a power of 100 mW. Open triangles and squares represent average values of J_{sc}^{norm} and V_{oc} , respectively. The dashed line is a guide for the eye.

transferred to the polymer and is delivered to the ITO electrode through the percolated network of conjugated polymer chains. Charge separation as described above occurs only if the NC-polymer forms a type II heterojunction. According to data in Fig. 1, in the case of P3HT type-II alignment is achieved for NC sizes smaller than 8 nm. Open-circuit-voltage data in Fig. 3(b) indicate that V_{oc} increases as the NC band gap is increased. The open-circuit voltage is 0.15 V for $E_g = 0.40$ eV (NC mean diameter is 10nm) and reaches a maximum of 0.49 V at $E_g = 0.81$ eV (NC mean diameter is 5 nm).

Figure 4 shows the incident photon conversion to electron (IPCE) spectrum under photovoltaic conditions (zero bias), as well as the absorption spectra of PbSe NCs for three different NC diameters. All of the devices show IR response due to exciton formation in the NC followed

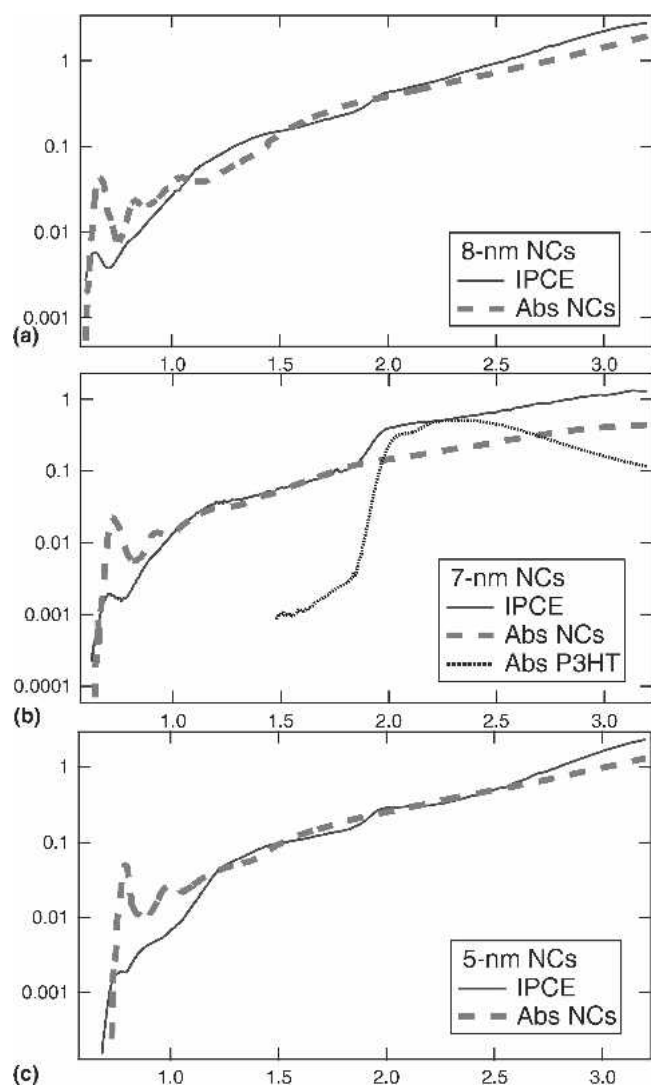


FIG. 4. Comparison between IPCE (solid lines) of RR-P3HT/PbSe-NC composite films and PbSe NC absorption spectra (dashed line) for indicated PbSe NC diameters. The absorption spectrum of RR-P3HT is also shown as a dotted line in (b).

by charge separation with hole transfer to the polymer. Photoresponse as far to the IR as 2 μm is observed. The IPCE and NC absorption spectra roughly correlate with each other over the entire spectral range studied. The IPCE onset is situated approximately at the position of the lowest-energy exciton absorption feature for all of the samples in Fig. 4. Contribution from the polymer is manifested as a step at ~ 2 eV, which is most pronounced in Fig. 4(b) (in this panel we also show the absorption spectrum of neat RR-P3HT for comparison) due to, probably, slightly more polymer composition in that device. These observations indicate that light absorption in the NC component of the structure plays a very important role in the device performance, especially in the IR range and the higher energy (>2.5 eV) part of the spectrum.

The photodiode response of devices consisting of RR-P3HT and PbSe NCs are shown in Fig. 5 for two NC sizes. It can be seen that the application of reverse bias to the devices causes a significant increase in the spectrally resolved photocurrent with nearly two-orders of magnitude increase of current for low photon energies. The low-energy onset of the photodiode response is also observed to depend upon the NC band gap as in the case of the photovoltaic response.

An interesting question is whether the performance of the structures studied here was affected by carrier multiplication. Spectroscopic investigations of this process indicate that in PbSe NCs it occurs at energies greater than approximately $3E_g$.² Above the $3E_g$ threshold, the internal quantum efficiency (IQE) for converting photons into charge carriers increases almost linearly with a slope of $\sim 114\%/E_g$ until it reaches $\sim 700\%$ (seven excitons per absorbed photon) at $7.8E_g$.^{32,33} In the experiments reported here, the IPCE values were measured up to $\sim 8E_g$.

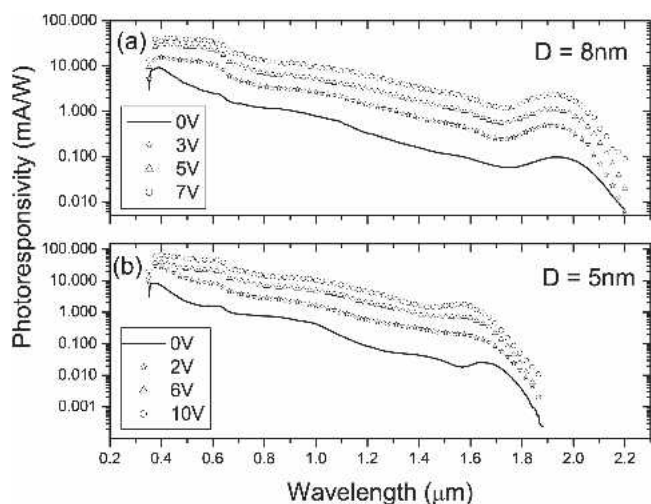


FIG. 5. Comparison of spectral responsivity of RR-P3HT/PbSe-NC devices under applied bias for (a) 8-nm diameter and (b) 5-nm diameter PbSe NCs. The rapid drop of responsivity near $0.38 \mu\text{m}$ is due to ITO absorption.

Therefore, carrier multiplication could in principle contribute to the photogenerated current. This additional contribution is expected to lead to a faster growth of IPCE compared to absorption above the threshold for multiexciton generation. However, in our experiments, we observed close correspondence between absorption and IPCE spectra across the entire range of spectral energies studied here, indicating that multiexcitons did not provide any noticeable contribution to the measured photocurrent. This result is not surprising given that extraction of multiexcitons from the NCs represents a significant challenge. Two specific complications in this case arise from very short multiexciton lifetimes (tens to hundreds of picoseconds) limited by nonradiative Auger recombination^{2,34} and a potential effect of NC charging. To take advantage of multiexciton generation, one needs to develop device architectures that would provide high charge-transfer rates (exceeding those of the Auger decay) in the case of both neutral and charged NCs. In non-optimized NC/polymer blends studied in this work, charge separation was likely not sufficiently fast to compete with the Auger recombination of multiexcitons. Observations of electron transfer rates of a few to tens of picoseconds have been reported^{35,36} between CdS NCs and TiO_2 . It was also shown that Auger rates can be suppressed via shape control,³⁷ though the effect of NC shape on CM efficiency is still being explored. Removal of the passivating layer was shown to promote charge transfer.³⁸

In general, regarding the hybrid system of polymer and NCs, there are two strategies that can be used to improve photovoltaic performance: one is to form more homogeneous bulk heterojunctions, and the other is to separate polymer and NC phase completely as in a bi-layer structure. The first has an advantage of rapid charge separation for excitons created in any dot; and the second one may help improve transport within the NC phase (refer, for example, to Murray's paper on mobilities in pure-quantum-dot films of order 10^{-1} in Ref. 39).

IV. CONCLUSION

In conclusion, we report studies of nanocomposites of conjugated polymer (RR-P3HT or MEH-PPV) with IR-sensitive PbSe NCs. Thin film cells show good diode characteristics and sizable photovoltaic response with an open circuit voltage of ~ 0.3 – 0.4 V, short circuit currents of ~ 0.2 mA/cm², and a power conversion efficiency of 0.04%. Photovoltaic response is observed throughout near-IR to 2 μm (0.6 eV), which is desirable for efficient utilization of both the IR and UV regions of the solar spectrum. Devices composed of RR-P3HT show a better photovoltaic performance than those made from MEH-PPV. This observation is consistent with results of CV studies of PbSe NCs, which indicate that the combination

of PbSe NCs with MEH-PPV does not provide a type-II alignment of electronic states. The reported devices did not show any contribution from multi-excitons to the photogenerated current, while spectroscopic studies show clear signatures of high-efficiency carrier multiplication in PbSe NCs in the spectral range studies in this work. The lack of carrier-multiplication-induced enhancement in the photovoltaic performance was likely because charge separation at the NC/polymer interface was not fast enough to compete with Auger recombination of multi-excitons.

ACKNOWLEDGMENTS

The authors thank the Air Force Office of Scientific Research for the financial support of this work (F49620-03-1-164), the Chemical Sciences, Biosciences and Geosciences Division of the Office of Basic Energy Sciences, Office of Science, United States Department of Energy, and Los Alamos Laboratory Directed Research and Development (LDRD) funds.

REFERENCES

- C.B. Murray, D.J. Norris, and M.G. Bawendi: Synthesis and characterization of nearly monodisperse CdE (E = sulfur, selenium, tellurium) semiconductor nanocrystallites. *J. Am. Chem. Soc.* **115**, 8706 (1993).
- R.D. Schaller and V.I. Klimov: High-efficiency carrier multiplication in PbSe nanocrystals: Implications for solar energy conversion. *Phys. Rev. Lett.* **92**, 186601 (2004).
- R.D. Schaller, M.A. Petruska, and V.I. Klimov: Effect of electronic structure on carrier multiplication efficiency: Comparative study of PbSe and CdSe nanocrystals. *Appl. Phys. Lett.* **87**, 253102 (2005).
- W. Shockley and H.J. Queisser: Detailed balance limit of efficiency of P-N junction solar cells. *J. Appl. Phys.* **32**, 510 (1961).
- V.I. Klimov: Detailed-balance power conversion limits of nanocrystal-quantum-dot solar cells in the presence of carrier multiplication. *Appl. Phys. Lett.* **89**, 123118 (2006).
- N.C. Greenham, X. Peng, and A.P. Alivisatos: Charge separation and transport in conjugated-polymer/semiconductor-nanocrystal composites studied by photoluminescence quenching and photoconductivity. *Phys. Rev. B* **54**, 17628 (1996).
- D.S. Ginger and N.C. Greenham: Charge injection and transport in films of CdSe nanocrystals. *J. Appl. Phys.* **87**, 1361 (2000).
- W.U. Huynh, J.J. Dittmer, and A.P. Alivisatos: Hybrid nanorod-polymer solar cells. *Science* **295**, 2425 (2002).
- W.U. Huynh, J.J. Dittmer, W.C. Libby, G.L. Whiting, and A.P. Alivisatos: Controlling the morphology of nanocrystal-polymer composites for solar cells. *Adv. Funct. Mater.* **13**, 73 (2003).
- J. Liu, T. Tanaka, K. Sivula, A.P. Alivisatos, and J.M.J. Frechet: Employing end-functional polythiophene to control the morphology of nanocrystal-polymer composites in hybrid solar cells. *J. Am. Chem. Soc.* **126**, 6550 (2004).
- B. Sun, E. Marx, and N.C. Greenham: Photovoltaic devices using blends of branched CdSe nanoparticles and conjugated polymers. *Nano Lett.* **3**, 961 (2003).
- P. Landsberg: *Recombination in Semiconductors* (Cambridge Univ. Press, Cambridge, UK, 1991).
- Next Generation Photovoltaics: High Efficiency through Full Spectrum Utilization*, edited by A. Marti and A. Luque (IOP Publishing, Bristol, 2004).
- C.B. Murray, S.H. Sun, W. Gaschler, H. Doyle, T.A. Betley, and C.R. Kagan: Colloidal synthesis of nanocrystals and nanocrystal superlattices. *IBM J. Res. Dev.* **45**, 47 (2001).
- J.M. Pietryga, R.D. Schaller, D. Werder, M.H. Stewart, V.I. Klimov, and J.A. Hollingsworth: Pushing the band gap envelope: Mid-infrared emitting colloidal PbSe quantum dots. *J. Am. Chem. Soc.* **126**, 11752 (2004).
- A.A. Guzelian, U. Banin, A.V. Kadavanich, X. Peng, and A.P. Alivisatos: Colloidal chemical synthesis and characterization of InAs nanocrystal quantum dots. *Appl. Phys. Lett.* **69**, 1432 (1996).
- A.L. Rogach, M.T. Harrison, S.V. Kershaw, A. Kornowski, M.G. Burt, A. Eychmuller, and H. Weller: Colloidally prepared CdHgTe and HgTe quantum dots with strong near-infrared luminescence. *Phys. Status Solidi* **224**, 153 (2001).
- S.A. McDonald, G. Konstantatos, S. Zhang, P.W. Cyr, E.J.D. Klem, L. Levina, and E.H. Sargent: Solution-processed PbS quantum dot infrared photodetectors and photovoltaics. *Nat. Mater.* **4**, 138 (2005).
- A. Maria, P.W. Cyr, E.J.D. Klem, L. Levina, and E.H. Sargent: Solution-processed infrared photovoltaic devices with >10% monochromatic internal quantum efficiency. *Appl. Phys. Lett.* **87**, 213112 (2005).
- A.A.R. Watt, D. Blake, J.H. Warner, E.A. Thomsen, E.L. Tavenner, H. Rubinsztein-Dunlop, and P. Meredith: Lead sulfide nanocrystal: Conducting polymer solar cells. *J. Phys. D* **38**, 2006 (2005).
- S. Zhang, P.W. Cyr, S.A. McDonald, G. Konstantatos, and E.H. Sargent: Enhanced infrared photovoltaic efficiency in PbS nanocrystal/semiconducting polymer composites: 600-fold increase in maximum power output via control of the ligand barrier. *Appl. Phys. Lett.* **87**, 233101 (2005).
- R. Plass, S. Pelet, J. Krueger, M. Gratzel, and U. Bach: Quantum dot sensitization of organic-inorganic hybrid solar cells. *J. Phys. Chem. B* **106**, 7578 (2002).
- X. Jiang, S.B. Lee, I.B. Altfeder, A.A. Zakhidov, R.D. Schaller, J.M. Pietryga, and V.I. Klimov: Nanocomposite solar cells based on conjugated polymer/PbSe quantum dot. *Proc. SPIE* **5938**, 59381F-1 (2005).
- D. Cui, J. Xu, T. Zhu, G. Paradee, S. Ashok, and M. Gerhold: Harvest of near infrared light in PbSe nanocrystal-polymer hybrid photovoltaic cells. *Appl. Phys. Lett.* **88**, 183111 (2006).
- D. Qi, M. Fischbein, M. Drndic, and S. Selmic: Efficient polymer-nanocrystal quantum-dot photodetectors. *Appl. Phys. Lett.* **86**, 093103 (2005).
- B.L. Wehrenberg and P. Guyot-Sionnest: Electron and hole injection in PbSe quantum dot films. *J. Am. Chem. Soc.* **125**, 7806 (2003).
- S.K. Haram, B.M. Quinn, and A.J. Bard: Electrochemistry of CdS nanoparticles: A correlation between optical and electrochemical band gaps. *J. Am. Chem. Soc.* **123**, 8860 (2001).
- I.H. Campbell, T.W. Hagler, D.L. Smith, and J.P. Ferraris: Direct measurement of conjugated polymer electronic excitation energies using metal/polymer/metal structures. *Phys. Rev. Lett.* **76**, 1900 (1996).
- Y. Liu, M.A. Summers, C. Edder, J.M.J. Frechet, and M.D. McGehee: Using resonance energy transfer to improve exciton harvesting in organic-inorganic hybrid photovoltaic cells. *Adv. Mater.* **17**, 2960 (2005).
- O. Solomeshch, A. Kigel, A. Saschiuk, V. Medvedev, A. Aharoni,

- A. Razin, Y. Eichen, U. Banin, E. Lifshitz, and N. Tessler: Photoelectronic properties of polymer-nanocrystal composites active at near-infrared wavelengths. *J. Appl. Phys.* **98**, 074310 (2005).
31. A.L. Efros and B.I. Shklovskii: Coulomb gap and low temperature conductivity of disordered systems. *J. Phys. C* **8**, L49 (1975).
32. R.D. Schaller, V.M. Agranovich, and V.I. Klimov: High-efficiency carrier multiplication through direct photogeneration of multi-excitons via virtual single-exciton states. *Nature Phys.* **1**, 189 (2005).
33. R.D. Schaller, M. Sykora, J.M. Pietryga, and V.I. Klimov: Seven excitons at a cost of one: Redefining the limits for conversion efficiency of photons into charge carriers. *Nano Lett.* **6**, 424 (2006).
34. V.I. Klimov, A.A. Mikhailovsky, D.W. McBranch, C.A. Leatherdale, and M.G. Bawendi: Quantization of multiparticle auger rates in semiconductor quantum dots. *Science* **287**, 1011 (2000).
35. J.E. Evans, K.W. Springer, and J.Z. Zhang: Femtosecond studies of interparticle electron transfer on a coupled CdS-TiO₂ colloidal system. *J. Chem. Phys.* **101**, 6222 (1994).
36. J.L. Blackburn, D.C. Selmarten, and A.J. Nozik: Electron transfer dynamics in quantum dot/titanium dioxide composites formed by in situ chemical bath deposition. *J. Phys. Chem. B* **107**, 14154 (2003).
37. H. Htoon, J.A. Hollingsworth, R. Dickerson, and V.I. Klimov: Effect of zero- to one-dimensional transformation on multiparticle auger recombination in semiconductor quantum rods. *Phys. Rev. Lett.* **91**, 227401 (2003).
38. W.U. Huynh, J.J. Dittmer, and A.P. Alivisatos: Hybrid nanorod-polymer solar cells. *Science* **295**, 2425 (2002).
39. D.V. Talapin and C.B. Murray: PbSe Nanocrystal solids for n- and p-channel thin film field-effect transistor. *Science* **310**, 86 (2005).